

assumption is consistent with all the available information. Taken together, the three sections provide evidence that about 120,000 years ago the mean inclination of the geomagnetic field was, for perhaps 20,000 years, steeper than that of the geocentric axial dipole (12).

This conclusion has important implications for our understanding of the geomagnetic field. If the field can sustain a steep inclination for tens of thousands of years, it is likely that it can sustain shallow inclinations for long periods as well. Such a conclusion supports the view that the shallow inclinations seen in late Glacial and Holocene sediments represent actual behavior of the geomagnetic field. It also suggests that it may be feasible to subdivide the Brunhes normal polarity epoch on the basis of whether the mean inclinations are steeper or shallower than the geocentric axial dipole value.

Equally important, if, over the past 35,000 years, the mean inclination of the geomagnetic field has been shallower than that of the geocentric axial dipole, then the time required for the field to average to such a dipole may be substantially greater than the 10,000- to 25,000-year interval now assumed to be required. Nongeocentric, axial components of the field may persist for 50,000 to 100,000 years, and the time required to average to a geocentric axial dipole field may be several hundred thousand years. In fact, paleomagnetic data from sequences of lava flows have been interpreted as showing that the geomagnetic field averages to an offset axial dipole rather than a geocentric dipole (13). All paleomagnetic determinations of the apparent motion of plates and microplates depend on the assumption that the paleomagnetic samples represent enough time for the field to have averaged to a geocentric axial dipole. If this time is significantly longer than has been assumed, or if it does not exist at all, then the results of some of these determinations will require reevaluation.

KENNETH L. VEROSUB

Department of Geology,
University of California,
Davis 95616

References and Notes

1. K. L. Verosub, *Rev. Geophys. Space Phys.* **15**, 129 (1977).
2. C. R. Denham and A. V. Cox, *Earth Planet. Sci. Lett.* **13**, 181 (1971).
3. K. L. Verosub, *ibid.* **36**, 219 (1977).
4. A. V. Cox, *Rev. Geophys. Space Phys.* **13**, 35 (1975).
5. D. E. Marchand and A. Allwardt, *U.S. Geol. Surv. Bull.* **1470** (1981).
6. J. Rosholt, personal communication.
7. R. O. Hansen and C. L. Begg, *Earth Planet. Sci. Lett.* **8**, 411 (1970).
8. The initial intensities of samples from sections A and B ranged from 1×10^{-4} to 1×10^{-5} EMU/cm³. On demagnetization, the intensity of each sample decreased continuously and smoothly and the median destructive fields ranged from 100 to 150 Oe. This behavior led me to infer that the magnetic carrier was magnetite, a conclusion confirmed by studies of the acquisition of a saturation-induced remanent magnetization. The intensities of the samples from section C were about an order of magnitude less than those of sections A and B, and the median destructive fields were between 200 and 300 Oe. The carrier was again inferred to be magnetite.
9. R. F. King, *Mon. Not. R. Astron. Soc. Geophys. Suppl.* **7**, 115 (1955).
10. K. L. Verosub and P. J. Mahringer, *Eos* **62**, 852 (1981).
11. K. M. Creer and P. Tucholka, *Can J. Earth Sci.* **19**, 1106 (1982).
12. There have been relatively few studies of secular variation in sediments 50,000 to 250,000 years old. Furthermore, the uncertainties in dating sediments in this age range make it impossible to determine whether any other sequence is contemporaneous with the Riverbank Formation.
13. C. G. A. Harrison and N. D. Watkins, *J. Geophys. Res.* **84**, 627 (1979).
14. J. L. Holloway, *Adv. Geophys.* **4**, 351 (1958).
15. I thank R. Shlemon and the late D. Marchand for sharing with me their understanding of late Quaternary sediments in the Sacramento and San Joaquin valleys. P. Waterstraat developed the computer programs used to analyze the data. Supported by NSF grant EAR-78-23559.

16 November 1982; revised 14 March 1983

Entwined and Parallel Bundled Orbits as Alternative Models for Narrow Planetary Ringlets

Abstract. *Particle orbits can be bundled in two different ways to produce narrow, Uranus-type ringlets. The usual assumption is that they are packed in a parallel manner in a structure that is essentially only two-dimensional, but it is then difficult to explain the large numbers of particles per unit area of the ring plane that are inferred from the observations. The alternative of a bundle of entwined orbits produces a three-dimensional structure of potentially large projected areal density. A start has been made in identifying possible mechanisms for stabilizing these structures, but much remains to be done, particularly for the less-studied model of entwined orbits. The two models might be discriminated observationally by differences in the motion of the line of intersection of the orbital and equatorial planes, and by the predicted radial reversal (entwined) or nonreversal (parallel) of features in occultation signatures taken at certain longitudes.*

The individual rings of Uranus are very narrow in their radial extent (1), and similar ringlets are embedded in the ring system of Saturn (2). There are two fundamentally different ways of bundling a large number of elliptical orbits to produce narrow, dense, and collisionless planetary ringlets. In a "parallel" arrangement, the radial order of orbits is the same at all longitudes. Nearly all the literature on rings is restricted, explicitly or implicitly, to the fundamental properties of this model (3). However, an "entwined" arrangement of the elliptical orbits is also possible, as described by Michel (4) and as treated independently by Eshleman *et al.* (5). Here the radial order changes with longitude and can even be reversed. For example, a particle on the inner edge of the entwined ringlet at one longitude is on the outer edge at another, making one clockwise or counterclockwise twist relative to the ringlet core during each circuit of the planet.

A successful model must explain the large observed optical depths, which can range to values so high that they indicate more area of particles projected into the average ring plane than there is ring plane area. It must explain ringlets that are both eccentric and inclined, since French *et al.* (6) found that the ringlets of Uranus are so disposed. And it must

account for the apparent long-term stability of its structure in the face of perturbing forces. In this report the two models are compared on these points to the limited degree allowed by their corresponding states of development. Some new material on their general structures is also presented.

The orbit and position of each ring particle is given by six parameters: a , e , i , ω , Ω , and f , representing, respectively, the semimajor axis and eccentricity of the elliptical orbit, its inclination relative to the planet's equatorial plane, the argument of periapsis or angle between the intersection (line of nodes) of the orbital and equatorial planes and the major axis or line of apsides (from the greatest orbital radius at apoapsis to smallest radius at periapsis) of the orbit, the longitude of the ascending node or angle between an inertial reference direction in the equatorial plane and the line of nodes, and the true anomaly or angle between the line of apsides and the radius vector of the particle. Although the possible arrays of these parameters for planetary ringlets are without limit, it appears that the two models can be characterized by just two sets.

For both models, it is assumed that particles are spread around each orbit with average separations proportional to their speeds, so that f is approximately

randomized. A filled orbit intersects the meridional plane at direct longitude ϕ from periapsis, at cylindrical coordinates

$$\begin{aligned} \rho &\cong a(1 - e \cos \phi) \\ z &\cong ai \sin(\phi + \omega) \end{aligned} \quad (1)$$

where ρ is the radial distance from the planet's spin axis, z is measured north of the equatorial plane, and the approximations are for small e and i carried to first order. In terms of the cylindrical azimuthal coordinate ϕ' measured from the same inertial direction as is Ω , note that $\phi' \cong \phi + \omega + \Omega$.

Let the above orbit be the core orbit of a ringlet consisting of many other filled orbits that extend in the other parameters by individual amounts given by δa , δe , δi , $\delta \omega$, and $\delta \Omega$. To lowest order, they intersect the meridional plane at

$$\begin{aligned} \Delta \rho &\cong \delta a - (a\delta e + e\delta a) \cos \phi \\ &\quad - ae(\delta \omega + \delta \Omega) \sin \phi \\ \Delta z &\cong (a\delta i + i\delta a) \sin(\phi + \omega) \\ &\quad - ai\delta \Omega \cos(\phi + \omega) \end{aligned} \quad (2)$$

relative to Eq. 1 for the core orbit. A number of the basic characteristics of the two ringlet models are available from Eq. 2 when the parameters are restricted

so that none of the filled orbits intersect.

The two models can be discriminated, at least partially, on the basis of whether $(\delta a)^2$ is greater or less than the sum of the squares of the maxima of the other two terms for $\Delta \rho$ in Eq. 2, for every pair of filled orbits in a ringlet. A sufficient condition for the parallel model is that $(\delta a)^2$ be greater, and a necessary condition for the entwined model is that it be less.

In Fig. 1 the intersections of representative "tracer" orbits with four meridional planes (spaced 90° in ϕ) are displayed in ρ - a , z coordinates. For the simplest parallel model of a ringlet with finite e and i , δe , δi , $\delta \omega$, and $\delta \Omega$ are all zero, while for a corresponding entwined model, δa and $\delta \omega$ are zero. These conditions are assumed in Fig. 1, along with the other parameters indicated in the legend.

Two key limitations of the models are illustrated in Fig. 1. The parallel model is inherently two-dimensional while the entwined model is three-dimensional. Note that the added tracer orbit represented by the cross is below the parallel ringlet plane at periapsis and above it at apoapsis, so it must pass through the main ring

plane, where collisions may occur. The added tracer orbit for the entwined model, on the other hand, can simply participate in the entwining without collisions. Dimensionality might be described as being in f - a space for the parallel model and in f - e - Ω space for the entwined model. While there can and sometimes must be variations of other parameters for both models, they are governed by these independent dimensions for collisionless structures. The other principal limitation is for the entwined model at arguments of periapsis ω near 90° and 270° , where the meridional cross section of the ringlet collapses to a line under conditions in which collisions could occur. More complex entwined models collapse in a different manner, but the problem of collapse is general. Thus it appears that valid parallel models are restricted to essentially two-dimensional structures and that the three-dimensional entwined models must somehow avoid values of ω near 90° and 270° .

The two alternative models for a somewhat more general ringlet are illustrated in Fig. 2, where the coordinates are now $\Delta \rho$ and Δz relative to the core orbit. Radial dimensions similar to those of the ϵ ring of Uranus (7) are used, as indicated. Note that the meridional cross sections vary in radial width with longitude ϕ and tilt both ways relative to the mean plane of the ringlet.

Ring models based on Earth-based observations of Saturn (8) differ from the dynamic parallel models (3) in that they are many particles thick instead of being confined very nearly to a plane. Voyager radio occultation data on Saturn's rings appear to be incompatible with a monolayer, although they do imply remarkable thinness (9). The entwined model tends to be favored from these considerations. In addition, large optical depths are easier to explain with the three-dimensional entwined model than with the parallel model. For example, the maximum observed optical depth of the ϵ ring of Uranus exceeds 2 (7), while it is difficult to obtain theoretical values much in excess of 1 for planar or parallel models.

On the other hand, the parallel model provides a more natural way of explaining the variable radial width of the ϵ ring, since Nicholson *et al.* (7) found that the inner and outer edges closely match Keplerian ellipses. In addition, the parallel model for the ϵ ring is supported by the very similar structure of the occultation signatures taken at several different longitudes and times (7). But care must be taken in interpreting a limited set of data. Whereas occultation profiles of the

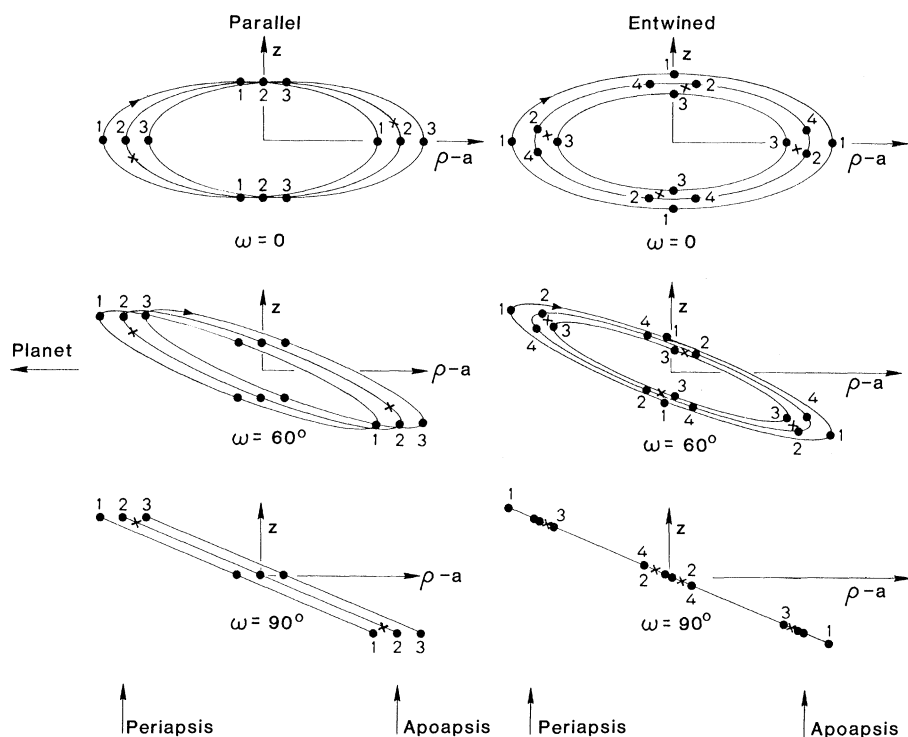


Fig. 1. Intersections of representative tracer orbits for parallel and entwined model ringlets with meridional planes at ringlet periapsis and apoapsis and at the two intermediate quadratures. The planet is far to the left. For both cases the core orbit has $e = 2.4i \ll 1$. For the parallel model, number 2 is the core orbit and orbits 1 and 3 have $\delta a = \pm ae/6$. For the entwined model, orbits 1 and 3 have $\delta e/e = \delta i/i = \pm 1/6$ and $\delta \Omega = 0$, while for orbits 2 and 4, $\delta e = \delta i = 0$ and $\delta \Omega = \mp 1/6$, respectively. The entwined core orbit is not shown, but it would be on the trajectory for orbits 2 and 4 and midway between them with $\delta \Omega = 0$. For $0 < \omega < 90^\circ$ the progression of the intersections with ϕ is clockwise (CW) in a CW-tilted figure, as illustrated for $\omega = 60^\circ$. It is counterclockwise (CCW) in a CW-tilted figure for $90^\circ < \omega < 180^\circ$, CCW in a CCW-tilted figure for $180^\circ < \omega < 270^\circ$, and CW in a CCW-tilted figure for $270^\circ < \omega < 360^\circ$.

entwined model in Fig. 2 would be reversed radially at $\phi = 0^\circ$ and 180° , they are generally not reversed at other opposite longitudes. Also, a concentration of orbits near tracer 1, for example, would be beyond the radial midpoint of the model ringlet for nearly 75 percent of the longitudes or times.

However, the major problem concerns how either model could maintain its integrity as an isolated and individual structure in the face of extrinsic perturbing forces. Only those forces due to the oblateness of the planet are discussed here, since some comparative work is available for the two models (10). For a single ring particle, $\dot{\omega}$ and $\dot{\Omega}$ change with time in such a way that $\dot{\omega} \cong -2\dot{\Omega} \sim a^{-7/2}$ because of oblateness. For the parallel model, in which a takes on a range of values, the differential changes in $\dot{\omega}$ and $\dot{\Omega}$ must be countered if the ringlet structure is to endure. For example, Goldreich and Tremain (11) showed that when $i = 0$, it is possible for the self-gravity of the particles to cause the ringlet to precess as a unit if its radial width is greater at apoapsis than at periapsis. For a similar parallel model ringlet that is inclined, the line that represents its meridional cross section cannot be radial if particle self-gravity is to prevent the destruction of the ringlet, since a force that is normal to the orbit planes is required to prevent the differential changes in $\dot{\Omega}$. In fact, what would be required is a value of δi that varies directly with δa and δe (and with $\delta e/e = \delta i/i$ for certain idealized conditions), as was assumed for the parallel model in Fig. 2. That is, at longitudes where the ringlet is above the equatorial plane, the outer edge of this cross section must be above the average plane of the ringlet, and vice versa. If the differential changes in $\dot{\omega}$ and $\dot{\Omega}$ are stopped by self-gravity, then the inclined parallel ringlet would endure and would have the same apsidal precession rate ($\dot{\omega} + \dot{\Omega}$) and the same nodal rate ($\dot{\Omega}$) as would the core orbit under the influence of the oblate planet alone.

For the model of entwined orbits, the differential effects can be near zero since the a 's of all the orbits can be the same. However, it is the direct changes in ω that cause the main problem here, as can be seen at the right in Fig. 1 for $\omega = 90^\circ$. Because collisions would then be expected to occur, it appears that this collapsed condition must be prevented if the ringlet is to endure. For an equatorial, hollow-shelled, circular ringlet consisting of entwined orbits, a complex but automatic state of stabilization against collapse has been found for electrically charged parti-

cles that display a small force of mutual repulsion (5). This produces alternating changes with time in both ω and i , but with $\dot{\omega} = 0$ on average and with the average value of ω being 0° or 180° . This type of effect has not yet been studied for more representative entwined models, but if they could be stabilized in a corresponding way, the entwined ringlet that does not collapse would have the same apsidal precession rate but the opposite average nodal rate as the core orbit alone. That is, the line of nodes would advance at the same average rate as the steady advance of the apsidal line, but would have a superposed fluctuation that might make it difficult to establish the average rate from a limited number of observations. French *et al.* (6) showed that stellar occultation observations for Uranus are consistent with the nodal regression rate that is predicted for the parallel model. However, since the test may be more sensitive to rate than to sign, this may not necessarily rule out the nodal advance, at the same average rate, that is predicted for the entwined model.

Although both models are still being developed, it appears that, in terms of certain major structural features, they represent the principal possibilities. Each has its advantages relative to the other. Particularly striking is the inherent advantage of the entwined model as a

three-dimensional structure. It also may be of special significance that an eccentric entwined ringlet could evolve to a final lossless state at a finite inclination, since it has only recently been realized that the narrow ringlets of Uranus are inclined (6). While this might also be possible for the parallel model, most theoretical literature has stressed the likelihood of an evolution to orbits of essentially zero inclination. The apparent "braided" structure of Saturn's F ring (2) is suggestive of the entwined model. For example, orbits 1 and 2 on the right in Fig. 1 might represent, instead of individual orbits, two separate entwined ringlets that are themselves mutually entwined. The initial development of the entwined model was largely due to the natural way that it might account for the W-shaped patterns observed in occultation measurements of the Saturn and Uranus ring systems (4, 5). As discussed, however, the rings of Uranus have other features that favor the parallel model. Although it seems unlikely that both models represent different actual ringlets, this remains a possibility. An even more bizarre possibility is that they both apply to a single ringlet having, for example, a core of large particles in parallel orbits and a halo of smaller particles in entwined orbits.

There are several possibilities for testing the applicability of the two models.

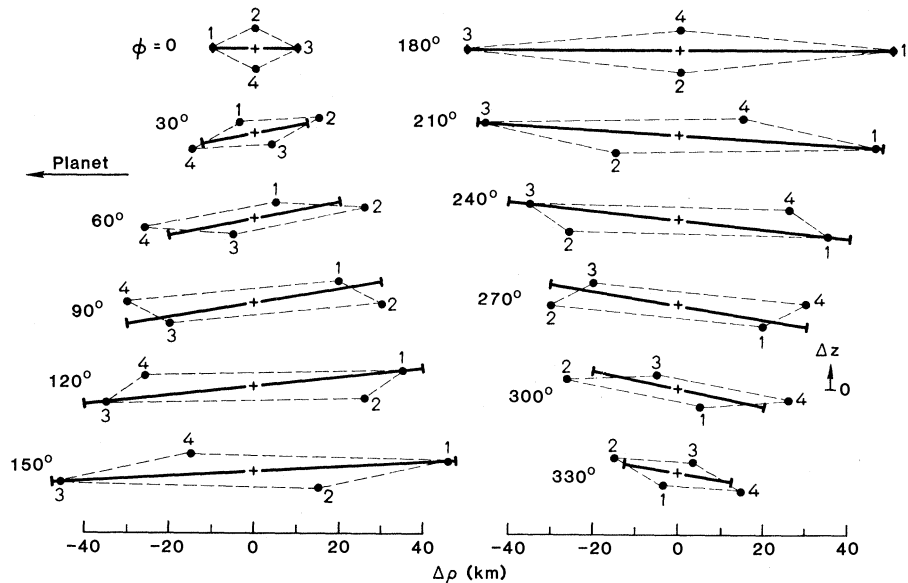


Fig. 2. Meridional cross sections of parallel and entwined models for approximations of the radial structure of the ϵ ring of Uranus. Results are given at 12 longitudes for zero argument of periapsis and the vertical dimensions (z , i , Δi) are exaggerated for clarity. For the core orbit $a = 5 \times 10^4$ m, $e = 8 \times 10^{-3}$, and $i = e/6$. Other parameters are chosen to produce radial widths of the ringlet at periapsis, quadrature, and apoapsis of 20, 60, and 100 km, respectively. For the parallel model the maximum magnitudes of $\delta a = 30$ km, $\delta \omega = \delta \Omega = 0$, and δe and δi are directly proportional to δa such that $\delta e = 2\delta a/3a$ and $\delta i = \delta a/6a$. The resultant meridional cross sections are shown as solid lines. For the entwined model, tracer orbits 1 and 3 have $\delta a = \pm 20$ km, $\delta e = \pm 6 \times 10^{-4}$, $\delta i = \pm 10^{-4}$, and $\delta \omega = \delta \Omega = 0$, while 2 and 4 have $\delta \Omega = \mp 3/40$ and $\delta a = \delta i = \delta e = \delta \omega = 0$.

Fine structure in the occultation signatures of a given parallel ringlet should occur in the same order in ρ for all longitudes, if the orbits are all filled. The entwined model, however, would generally show differences and under particular conditions, even a radial reversal. A parallel model that is stabilized by self-gravity must have a greater radial width at apoapsis than at periapsis and a characteristic longitudinal reversal in the tilt of the local plane of the ringlet relative to its average orbital plane. Neither characteristic is known to be required for the entwined model, although both are structural possibilities (Fig. 2). Finally, the nodal precessions for the two models would be markedly different if they were stabilized in the ways suggested above.

VON R. ESHLEMAN

Space, Telecommunications, and
Radioscience Laboratory,
Stanford University,
Stanford, California 94305

References and Notes

1. J. L. Elliot, E. Dunham, D. Mink, *Nature (London)* **267**, 328 (1977); R. L. Millis and L. H. Wasserman, *Astron. J.* **83**, 993 (1978); J. L. Elliot, E. Dunham, L. H. Wasserman, R. L. Millis, J. Churms, *ibid.*, p. 980; P. D. Nicholson, S. E. Persson, K. Matthews, P. Goldreich, G. Neugebauer, *ibid.*, p. 1240.
2. B. A. Smith *et al.*, *Science* **215**, 504 (1982); A. L. Lane *et al.*, *ibid.*, p. 537; B. R. Sandel *et al.*, *ibid.*, p. 548; G. L. Tyler, E. A. Marouf, R. A. Simpson, H. S. Zebker, V. R. Eshleman, *Icarus* **54**, 160 (1983).
3. H. Jeffreys, *Mon. Not. R. Astron. Soc.* **107**, 263 (1947); A. Brahic, *Astron. Astrophys.* **54**, 895 (1977); P. Goldreich, *Annu. Rev. Astron. Astrophys.* **20**, 249 (1982); P. Goldreich and S. Tremaine, *Icarus* **34**, 277 (1978); *ibid.*, p. 240; *Astrophys. J.* **233**, 857 (1979); *ibid.* **243**, 1062 (1981); J. A. Burns, P. Hamill, J. N. Cuzzi, R. H. Durisen, *Astron. J.* **84**, 1783 (1979); J. L. Elliot, R. G. French, J. A. Frogel, J. H. Elias, D. J. Mink, W. Liller, *ibid.* **86**, 444 (1981); P. D. Nicholson, K. Matthews, P. Goldreich, *ibid.*, p. 596; J. N. Cuzzi, R. H. Durisen, J. A. Burns, P. Hamill, *Icarus* **38**, 54 (1979).
4. F. C. Michel, *Planet. Space Sci.* **29**, 1137 (1981); *Astrophys. Lett.* **22**, 101 (1982).
5. V. R. Eshleman, J. V. Breakwell, G. L. Tyler, E. A. Marouf, *Icarus* **54**, 212 (1983). Tyler and Eshleman discussed aspects of the entwined model at two public meetings at the time of the Voyager 2 encounter of Saturn in August 1981.
6. R. G. French, J. L. Elliot, D. A. Allen, *Nature (London)* **289**, 827 (1982).
7. P. D. Nicholson, K. Matthews, P. Goldreich, *Astron. J.* **87**, 433 (1982).
8. J. B. Pollack, *Space Sci. Rev.* **18**, 3 (1975); J. N. Cuzzi and J. B. Pollack, *Icarus* **33**, 233 (1978); J. N. Cuzzi, J. B. Pollack, A. L. Summers, *ibid.* **44**, 683 (1980); E. E. Epstein, M. A. Janssen, J. N. Cuzzi, W. G. Fogarty, J. Mortman, *ibid.* **41**, 103 (1980).
9. E. A. Marouf, G. L. Tyler, H. A. Zebker, R. A. Simpson, V. R. Eshleman, *Icarus* **54**, 189 (1983); E. A. Marouf, G. L. Tyler, V. R. Eshleman, *ibid.* **49**, 161 (1982); H. A. Zebker, G. L. Tyler, E. A. Marouf, in preparation; H. A. Zebker, private communication.
10. Satellite perturbations, particularly those of nearby "shepherding" satellites (1), are potentially important for ringlet stability, but it has not been established whether the narrow ringlets generally have such shepherds.
11. P. Goldreich and S. Tremaine, *Nature (London)* **277**, 97 (1979); *Astron. J.* **84**, 1638 (1979).
12. This work was supported by NASA. I thank J. V. Breakwell, E. A. Marouf, G. L. Tyler, P. D. Nicholson, and R. G. French for helpful discussions.

11 January 1983; revised 28 March 1983

Miocene Burrows of Extinct Bear Dogs: Indication of Early Denning Behavior of Large Mammalian Carnivores

Abstract. *Partial skeletons of four species of extinct carnivores have been found in their dens excavated in the floodplain of an early Miocene ephemeral braided stream at Agate Fossil Beds National Monument, Nebraska. Bear dogs (Carnivora: Amphicyonidae) were the principal occupants; their den dimensions and body size are similar to those of living wolves and hyenas. Discovery of this predator community extends the record of denning behavior of large mammalian carnivores to the early Miocene, 20 million years ago.*

Relatively complete fossil skeletons of mammals preserved directly in their ancient environment provide insight into mammalian paleoecology. We report the discovery of a 20-million-year-old den complex (1) with partial skeletons of four species of extinct Miocene Carnivora. The remains, found in burrow fills over 30 m² in the floodplain of an early Miocene ephemeral stream, are an unusual occurrence in the fossil record (2).

The discovery extends the age of denning behavior of large terrestrial Carnivora to the early Miocene. It also indicates that amphicyonid carnivores (the dominant mid-Cenozoic land Carnivora) used dens and that denning was within the capability of many if not all amphicyonids, since species from two widely divergent lineages were found in separate dens (3). Furthermore, the skeletons in the den complex suggest that the dens were used in protection and care of the young and as shelter for adults; to our knowledge they provide the only evidence known in the Tertiary fossil record for the occupation of a den by a succession of carnivore species. The Agate den complex represents one of the oldest known burrow systems (4).

The history of this ancient predator community can be reconstructed from the size and form of the burrows, the ages of the carnivores (established by the degree of eruption and wear on teeth), the condition of the skeletons, and the nature of sediment fill. The form and large size of the burrows, similar to burrows of living large canids and hyaenids, suggest their construction or remodeling by the largest terrestrial carnivores of the early Miocene, the amphicyonids or bear dogs. The bear dogs found in the dens resemble wolves in size and certain skeletal features, but are not closely related. The bear dog *Daphoenodon superbus* is represented by at least six or seven individuals, and a rare temnocyonine bear dog by one skeleton. A juvenile, a mature adult, and at least three old individuals of *Daphoenodon* can be identified from dental evidence. Skeletal features indicate that the remains of one or

two other individuals, which are not represented by teeth, are adults. Although old individuals possibly died in the dens through normal attrition, the deaths of the juvenile and young adults in the burrows must have been premature and probably sudden. The partial disarticulation of all skeletons in the burrows and bite marks on some bones show that there was sufficient time for decomposition and scavenging of carcasses to take place before sediment burial.

In addition to bear dogs, the dens contained remains of small canid and mustelid carnivores. Because simultaneous occupation of a den by more than one species is uncommon among living Carnivora, the presence of more than one kind of fossil carnivore in these dens suggests they were used by a succession of species, that the smaller carnivores were occasional prey of the larger bear dogs, or both. However, the presence of only a few herbivore bone fragments within the burrows indicates that prey carcasses were infrequently taken into the dens, thus the small carnivores were probably den occupants.

The dens (Fig. 1) occur in an area 5 by 6 m in quarry 3 on Beardog Hill, Agate Fossil Beds National Monument, Nebraska. Carnivores burrowed into a stream channel fill of tuffaceous white fine-grained sandstone (Upper Harrison beds, Arikaree Group). Only 150 to 300 m north of the dens, this same sandstone contains the dense bone deposits of early Miocene rhinoceros, chalicothere, and entelodont, which were found at the national monument early in this century (5, 6). Thus the dens must postdate deposition of the principal Agate bone bed. The time that elapsed between formation of the great bone bed and the dens was probably brief in the perspective of geologic time, since fragments of the same carnivore species found in the dens have also been found in the bone bed (6, 7). These carnivores have short temporal ranges of at most a few million years. We suspect that the dens were emplaced only weeks to a few years after the Agate bone bed was deposited.